

Low-Complexity Random Rotation-based Schemes for Intelligent Reflecting Surfaces

Constantinos Psomas, *Senior Member, IEEE*, Ilias Chrysovergis, *Student Member, IEEE*, and Ioannis Krikidis, *Fellow, IEEE*

Abstract

The employment of intelligent reflecting surfaces (IRSs) is a potential and promising solution to increase the spectral and energy efficiency of wireless communication networks. The passive operation of their elements and the fact that they can be deployed on any flat surface, makes them ideal for both indoor and outdoor applications. On the other hand, the capabilities of IRS-aided communications have limitations as they are subject to high propagation losses. To overcome this, the phase rotation at each element needs to be designed in such a way as to increase the channel gain at the destination. However, this increases the system's complexity as well as its power consumption. In this paper, we present an analytical framework for the performance of random rotation-based IRS-aided communications. Under this framework, we propose four low-complexity and energy efficient techniques based on two approaches: a coding-based and a selection-based approach. Both approaches depend on random phase rotations and require no channel state information. In particular, the coding-based schemes use time-varying random phase rotations to produce a time-varying channel, whereas the selection-based schemes, select a partition of the IRS elements at each time slot based on the received signal power at the destination. Analytical expressions for the achieved outage probability and energy efficiency of each scheme are derived. It is demonstrated that all schemes can provide significant performance gains as well as full diversity order.

Index Terms

Intelligent reflecting surfaces, outage probability, energy efficiency, selection, diversity.

C. Psomas, I. Chrysovergis, and I. Krikidis are with the IRIDA Research Centre for Communication Technologies, Department of Electrical and Computer Engineering, University of Cyprus, Nicosia, Cyprus (e-mail: {psomas, chrysovergis.ilias, krikidis}@ucy.ac.cy).

I. INTRODUCTION

Despite the fact that the 5G-era has commenced, with its deployment in some countries, the challenge of how to connect billions of devices and satisfy their rate requirements still exists. Furthermore, the energy efficiency of such highly dense and highly connected wireless communication networks is another vital requirement of particular interest [1]. A promising new technology which aims to address these issues is the so-called intelligent reflecting surfaces (IRSs), also known as reconfigurable intelligent surfaces [2]. An IRS consists of an array of passive elements embedded in a flat metasurface, where each element is reconfigurable and can alter the phase of the incident signal with the help of a dedicated controller [3]. Thus, through these software-controlled reflections of the signals, a smart and programmable wireless environment can be achieved [4]. Their employment can provide many benefits such as extend the range of wireless communication systems, improve spectral efficiency by means of their full-duplex operation as well as increase energy efficiency due to the passive operation of their elements.

As a result, IRS-aided communications has recently attracted substantial attention by the research community and has already been investigated under various different communication scenarios [5]–[17]. Specifically, in [5], the authors study a single cell wireless system where a multi-antenna access point (AP) communicates with multiple users via an IRS; it is verified that by jointly optimizing the active beamforming from the AP and the passive beamforming from the IRS, provides performance gains. A similar scenario is considered in [6], where it is demonstrated that IRSs can outperform both half- and full-duplex amplify-and-forward relays. The implementation of two index modulation schemes, space shift keying and spatial modulation, in IRS-aided communications is studied in [7]. It is shown that good spectral efficiency performance can be achieved even for low signal-to-noise ratio (SNR) values. The authors in [8], consider IRS-assisted non-orthogonal multiple access (NOMA) communications and it is demonstrated that NOMA can benefit from the employment of IRSs. An upper bound for the ergodic spectral efficiency of an IRS-assisted system is evaluated in [9], and an optimal phase shift design is proposed to maximize the ergodic spectral efficiency. Moreover, the benefits from the employment of IRSs, in terms of physical layer security, are shown in [10] and [11]. In particular, the work in [10] designs the AP's transmit beamforming and the IRS's reflect beamforming, such that the transmit power is minimized subject to a secrecy rate constraint.

On the other hand, in [11], the authors jointly optimize the AP's transmit beamforming and the IRS's reflect beamforming in order to maximize the secrecy rate.

The energy efficiency of IRS deployments is investigated in [12], where the proposed resource allocation methods achieved up to 300% higher energy efficiency compared to the conventional multi-antenna amplify-and-forward relaying. In [13], the authors compare an IRS-aided system with the conventional decode-and-forward relaying in terms of rate and energy efficiency. It is shown that the IRS needs a large number of elements in order to compensate for the low channel gain. A stochastic geometry model with IRSs is presented in [14], where the spatial randomness of users is taken into account. The derived analytical framework for the spectral and energy efficiency of the proposed model validates the gains from the employment of multiple IRSs. The uplink data rate in an IRS system is considered in [15], where an asymptotic analysis is undertaken with imperfect channel estimation and correlated interference; it is shown that noise and interference from channel estimation errors become negligible as the number of elements increases. The implementation of IRSs has also been considered in the context of simultaneous wireless information and power transfer [16], [17]. Specifically, the work in [16], considers an IRS-aided wireless system with multiple information receivers and energy harvesters. By maximizing the weighted sum-power at the energy harvesters, it is demonstrated that IRS can enhance the performance. A similar scenario is considered in [17], where by maximizing the weighted sum-rate of the information receivers under certain energy harvesting constraints, it is shown that the existence of an IRS benefits the network.

Most of the aforementioned works, mainly focus on optimizing the incident signal's phase shifts at the IRS and assume knowledge of the channel state information. However, this corresponds to higher complexity and power consumption but can also be impractical in some cases. Motivated by this, in this paper, we present an analytical framework for the performance of random rotation-based IRS-aided communications. We propose four low-complexity and energy efficient techniques based on two approaches: a coding-based and a selection-based approach. Both approaches depend on random phase rotations and require no channel state information. Specifically, the main contributions of this work are

- A complete analytical framework for the performance of random rotation-based IRS schemes is presented; we consider both non-coherent and coherent (beamforming) cases. Building on this framework, we propose four schemes and derive analytical expressions for the outage probability and the energy efficiency. Furthermore, a diversity analysis is undertaken, where

we provide the achieved diversity order and array gain. Our results demonstrate that the proposed schemes can enhance the performance of IRS-aided communication systems both in terms of outage and energy efficiency.

- We propose a random rotations coding-based (RRC) scheme, inspired by the rotate-and-forward protocol [18], which produces a time-varying channel through time-varying random rotations. We show that RRC can achieve significant performance gains over a small number of channel uses, and provides full time diversity order. Furthermore, we present a coding-based one-bit feedback (OBF) scheme, which adjusts the phase rotation at each element according to a one-bit returned by the destination during a training period. It is demonstrated that, even for a short training period, the OBF scheme can improve performance. We show that as the training period increases, the algorithm converges to the beamforming case.
- Two selection-based schemes are proposed, which select a partition (sub-surface) of the IRS elements at each time slot based on the received signal power at the destination. In particular, the transmit diversity (TD) selects the sub-surface which provides the highest achieved SNR at the destination. It is shown that the TD scheme provides full spatial diversity order and can substantially increase the energy efficiency. On the other hand, the adaptive transmit diversity (ATD) scheme, selects a sub-surface which achieves an SNR which exceeds a certain threshold. The ATD scheme is of lower complexity compared to the TD but can still achieve full diversity order and improve the performance.

The rest of this paper is organized as follows: Section II describes the considered system model and presents our main assumptions. Section III provides preliminary analytical results for random rotation-based schemes. Then, in Section IV and Section V, we present the proposed coding-based and selection-based schemes, respectively, together with their analytical expressions. A discussion and some numerical results are provided in Section VI. Finally, the paper is concluded with Section VII.

Notation: Lower and upper case boldface letters denote vectors and matrices, respectively; $[\cdot]^T$ denotes the transpose operator and $O(\cdot)$ denotes the big O notation; $\Im(z)$ returns the imaginary part of z and $j = \sqrt{-1}$ denotes the imaginary unit; $\mathbb{P}\{X\}$ and $\mathbb{E}\{X\}$ represent the probability and the expectation of X , respectively; $\mathbb{1}_X$ is the indicator function of X with $\mathbb{1}_X = 1$ if X is true and $\mathbb{1}_X = 0$ otherwise; $K_M(\cdot)$ is the modified Bessel function of the second kind of order M , $\Gamma(\cdot)$ denotes the complete gamma function, $\log(\cdot)$ is the natural logarithm, and $\binom{n}{k} = \frac{n!}{(n-k)!k!}$ is the binomial coefficient.

II. SYSTEM MODEL

Consider an IRS-aided network, where a source S achieves communication with a destination D through the employment of an IRS with M reflecting elements, as shown in Fig. 1. The source and destination are equipped with a single antenna and a direct link between them is not available (e.g., due to obstacles). A codeword

$$\mathbf{x} \triangleq [x_1, x_2, \dots, x_T], x_t \in \mathbb{C}, 1 \leq t \leq T, \quad (1)$$

is transmitted by the source over T symbols time. All wireless links are assumed to exhibit Rayleigh fading; we define by h_i and g_i the fading coefficients from S to the i -th IRS element and from the i -th IRS element to D , respectively. The fading coefficients remain constant during the T transmissions but change independently every T channel uses according to a complex Gaussian distribution with zero mean and unit variance, i.e. $h_i \sim \mathcal{CN}(0, 1)$ and $g_i \sim \mathcal{CN}(0, 1)$.

We assume that knowledge of any channel state information does not exist. At every time instant t , each element of the IRS, randomly rotates (shifts) the phase of the incident signal. Denote by

$$\Phi_t = \text{diag}[\exp(j\phi_{t,1}) \exp(j\phi_{t,2}) \cdots \exp(j\phi_{t,M})], \quad (2)$$

the diagonal matrix containing the independent and identically distributed phase shift variables. Due to the random rotations, the variables $\phi_{t,i}$ are uniformly distributed in $[0, 2\pi)$. Therefore, if the source transmits with a constant power P , the received signal at the destination D at the t -th channel use can be written as

$$r_t = \sqrt{P} \mathbf{h}^\top \Phi_t \mathbf{g} x_t + n_t, \quad (3)$$

where $\mathbf{h} = [h_1 \ h_2 \ \cdots \ h_M]^\top$, $\mathbf{g} = [g_1 \ g_2 \ \cdots \ g_M]^\top$, and $n_t \sim \mathcal{CN}(0, \sigma^2)$ is the additive white Gaussian noise with variance σ^2 . Then, the instantaneous SNR at the destination D over the t -th transmission is

$$\gamma_t = \frac{P}{\sigma^2} H_t, \quad (4)$$

where

$$H_t = \left| \sum_{i=1}^M h_i g_i \exp(j\phi_{t,i}) \right|^2, \quad (5)$$

is the channel gain from the M elements of the IRS.

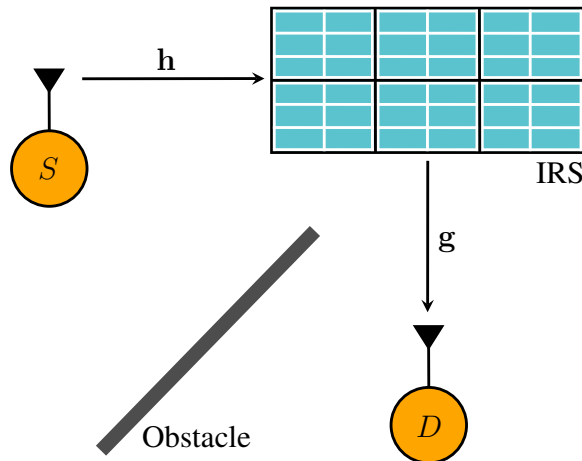


Fig. 1. The considered IRS-aided communication network.

III. RANDOM ROTATION-BASED SCHEMES: PRELIMINARIES

In this section, we describe the main performance metrics considered for each scheme, namely, the outage probability and the energy efficiency. In addition, we provide preliminary results, which will assist in the derivation of the main analytical results of this paper but will also serve as benchmarks to our proposed schemes.

Let ρ be a non-negative pre-defined threshold. Then,

$$\Pi(\rho, T) = \mathbb{P} \left\{ \frac{1}{T} \sum_{t=1}^T \log_2(1 + \gamma_t) < \rho \right\}, \quad (6)$$

defines the achieved outage probability over T channel uses. Moreover, the end-to-end energy efficiency, measured in bits per Joule, is written as

$$\eta = \frac{\mathbb{E} \left\{ \frac{1}{T} \sum_{t=1}^T \log_2(1 + \gamma_t) \right\}}{P_c}, \quad (7)$$

where $\mathbb{E} \left\{ \frac{1}{T} \sum_{t=1}^T \log_2(1 + \gamma_t) \right\}$ is the expected rate and P_c is the system's total power consumption. Finally, the diversity order of a scheme is given by

$$d = - \lim_{P \rightarrow \infty} \frac{\log(\Pi(\rho, T))}{\log(P)}. \quad (8)$$

We now state the following two propositions for the conventional case $T = 1$, with non-coherent (Proposition 1) and coherent transmissions (Proposition 2), which will be used as benchmarks to our proposed schemes.

Proposition 1. *The outage probability achieved by a random rotation of M elements with $T = 1$ is given by*

$$\Pi(\rho, 1) = 1 - \frac{2}{\Gamma(M)} \left(\frac{\theta\sigma^2}{P} \right)^{\frac{M}{2}} K_M \left(2\sqrt{\frac{\theta\sigma^2}{P}} \right), \quad (9)$$

where $\theta \triangleq 2^\rho - 1$.

Proof. See Appendix A. □

Proposition 2. *The outage probability achieved by a coherent transmission (beamforming) of M elements is given by*

$$\Pi_{\text{CT}}(\rho) = \frac{1}{\pi} \int_0^\infty \Im \left(\phi_H(t) \sum_{i=2M}^\infty (-1)^{i+1} \left(j\sqrt{\frac{\theta\sigma^2}{P}} \right)^i \frac{t^{i-1}}{i!} \right) dt, \quad (10)$$

where $\phi_H(t)$ is the characteristic function of H and is given by

$$\phi_H(t) = \left(\frac{4\sqrt{t^2 + 4} + 2j\pi t - 4t \sinh^{-1} \left(\frac{t}{2} \right)}{(t^2 + 4)^{3/2}} \right)^M, \quad (11)$$

where $\theta \triangleq 2^\rho - 1$.

Proof. See Appendix B. □

Finally, we provide the lemma below, which approximates the channel gain H_t as exponential random variables based on the central limit theorem (CLT).

Lemma 1. *Under the CLT, the channel gain H_t converges in distribution to an exponential random variable, with parameter $1/M$.*

Proof. See Appendix C. □

IV. CODING-BASED IRS SCHEMES

For the coding-based schemes, the destination receives the superposition of M independent channels at each time instant t . Following this approach, we propose two schemes: the RRC scheme, which employs random phase shifts at each channel use, and the OBF scheme, which implements a one-bit feedback protocol over a training period to increase the channel gain at the destination.

A. Random Rotations Coding-based Scheme

The different phase shifts induced by the IRS elements at each channel use, introduce an artificial fast fading channel. This can increase the performance [18], without any knowledge of channel state information. Note that the instantaneous channel gains between different channel uses are correlated, which makes the derivation of the outage probability challenging. As such, we present two approximations in the following two theorems. In particular,

- Theorem 1 provides an approximate mathematical expression by assuming that the channel gains H_t are mutually independent; it is proven analytically that as M increases, the correlation over different channel uses decreases.
- Theorem 2 approximates the outage probability using Lemma 1, which employs the CLT to approximate H_t as an exponential random variable; this results in a simpler analytical expression.

We show in Section VI that both approximations are sufficient and appropriate to describe the proposed scheme's behavior.

Theorem 1. *The outage probability of the RRC scheme, under the independence assumption, is approximated by*

$$\begin{aligned} \Pi_{\text{RRC}}^{\text{IND}}(\rho, T) \approx & \left(\frac{\sigma^2}{P}\right)^{T-1} \int_1^{\xi_T} \cdots \int_1^{\xi_2} \left(1 - \frac{2\Theta^{M/2}}{\Gamma(M)} K_M(2\sqrt{\Theta})\right) \\ & \times \prod_{t=2}^T f_H\left(\frac{\sigma^2}{P}(w_t - 1)\right) dw_2 \cdots dw_T, \end{aligned} \quad (12)$$

where $\xi_i = 2^{\rho T} / \prod_{t=i+1}^T w_t$, $2 \leq i \leq T$,

$$\Theta \triangleq \frac{\sigma^2}{P} \left(\frac{2^{\rho T}}{\prod_{t=2}^T w_t} - 1 \right), \quad (13)$$

and

$$f_H(h) = \frac{2h^{(M-1)/2} K_{M-1}(2\sqrt{h})}{\Gamma(M)}. \quad (14)$$

Proof. See Appendix D. □

It is clear that for the case $T = 1$, Theorem 1 corresponds to the exact analytical result in Proposition 1. Next, we derive the outage probability with the use of the CLT.

Theorem 2. *The outage probability of the RRC scheme, under the CLT, is approximated by*

$$\begin{aligned} \Pi_{\text{RRC}}^{\text{CLT}}(\rho, T) \approx & \left(\frac{\sigma^2}{MP}\right)^{T-1} \int_1^{\xi_T} \cdots \int_1^{\xi_2} \left(1 - \exp\left(-\frac{\Theta}{M}\right)\right) \\ & \times \prod_{t=2}^T \exp\left(-\frac{\sigma^2}{MP}(w_t - 1)\right) dw_2 \cdots dw_T, \end{aligned} \quad (15)$$

where Θ and ξ_i are given in Theorem 1.

Proof. By Lemma 1, the random variables H_t are independent of t . Hence, the final result can be derived by following similar steps to the proof of Theorem 1 with CDF $F_H(h) = 1 - \exp(-h/M)$ and PDF $f_H(h) = \exp(-h/M)/M$. \square

Remark 1. *Even though the theorems above are derived based on the assumption that M is large, they also work well for small M . Overall, Theorem 1 provides the best approximation for any value of M . On the other hand, Theorem 2, due to its simplest mathematical form, can provide further system insights by assisting in the derivation of the diversity order and array gain (see below). Finally, asymptotically ($M \rightarrow \infty$), both theorems produce the same results.*

We now turn our attention to the energy efficiency achieved by this scheme, as described by (7), which takes into account the achieved expected rate. Note that the expected rate of RRC is independent of T since

$$\mathbb{E} \left\{ \frac{1}{T} \sum_{t=1}^T \log_2(1 + \gamma_t) \right\} = \frac{1}{T} \sum_{t=1}^T \mathbb{E} \{ \log_2(1 + \gamma_t) \} = \mathbb{E} \{ \log_2(1 + \gamma_t) \}. \quad (16)$$

Thus, we can state the following.

Proposition 3. *The expected rate achieved by the RRC scheme is*

$$R_{\text{RRC}} = \frac{2}{\Gamma(M)} \int_0^\infty \left(\frac{\theta\sigma^2}{P}\right)^{\frac{M}{2}} K_M \left(2\sqrt{\frac{\theta\sigma^2}{P}}\right) d\rho, \quad (17)$$

where $\theta \triangleq 2^\rho - 1$.

Proof. The result follows simply from the fact that the expectation of a non-negative random variable X is given by $\mathbb{E}\{X\} = \int_{x>0} \mathbb{P}\{X > x\} dx$. Therefore, $R_{\text{RRC}} = \int_0^\infty \mathbb{P}\{\log_2(1 + \gamma_t) > \rho\} d\rho$, and the final expression is derived by the use of Proposition 1. \square

Then, from (7), we have that the energy efficiency achieved by the RRC scheme is

$$\eta_{\text{RRC}} = \frac{R_{\text{RRC}}}{P/\xi + P_S + P_D + P_{\text{IRS}}}, \quad (18)$$

where ξ is the amplifier's efficiency, whereas P_S , P_D and P_{IRS} is the static power consumption at the source, destination and IRS, respectively [12]. The power consumption at the IRS depends on the number of activated elements, that is, $P_{\text{IRS}} = MP_E$, where P_E is the power consumed to operate a single element.

B. One-bit Feedback Scheme

We now present a coding-based algorithm similar to the one proposed in [19], which is of low-complexity in terms of time and memory. The algorithm aims to achieve beamforming by adjusting the phase rotation at each element based on a one-bit feedback protocol, at each time instant, over a training period of duration $\tau \leq T$. The one-bit feedback from the destination to the IRS controller, dictates whether or not the change in the phase rotations has increased the received SNR compared to an SNR value γ_0 achieved at a previous channel use. Specifically, the algorithm follows the steps below for the first $\tau \leq T$ channel uses

- The destination sets the initial value of γ_0 at $t = 1$, i.e. $\gamma_0 = \gamma_1 = \frac{P}{\sigma^2} \left| \sum_{i=1}^M h_i g_i \exp(j\phi_{1,i}) \right|^2$, and the initial random rotations $\phi_{0,i} = \phi_{1,i} \in [0, 2\pi)$ set at the IRS controller.
- At each time instant $2 \leq t \leq \tau$, each element of the IRS rotates the phase of the received signal using the following update step

$$\phi_{t,i} = \phi_{0,i} + \delta_{t,i}, \quad \forall i \in \{1, \dots, M\}, \quad (19)$$

where $\delta_{t,i} \sim U[-\Delta, \Delta]$, $0 < \Delta \leq \pi$ and Δ is the maximum step size.

- If $\gamma_t > \gamma_0$, the destination returns a positive feedback and sets $\gamma_0 = \gamma_t$; otherwise, it sends a negative feedback and γ_0 remains unchanged. In turn, the IRS controller sets $\phi_{0,i} = \phi_{t,i}$ if it receives a positive feedback; otherwise, $\phi_{0,i}$ is not changed.

Then, at time instant $\tau + 1$, the IRS fixes the phase rotations at $\phi_{0,i}$ for the remaining $T - \tau$ channel uses. Based on the above, at time instant t , the rotation angle of the i -th IRS element is

$$\phi_{t,i} = \phi_{1,i} + \sum_{n=2}^t \delta_{n,i} \mathbb{1}_{\gamma_n > \gamma_0}, \quad (20)$$

while the channel gain at t is

$$H_t = \left| \sum_{i=1}^M h_i g_i \exp \left(j \left(\phi_{1,i} + \sum_{n=2}^t \delta_{n,i} \mathbb{1}_{\gamma_n > \gamma_0} \right) \right) \right|^2. \quad (21)$$

Note that, if there is no constraint on τ , the algorithm will converge to the optimal beamforming gain, regardless of the value for the maximum step size Δ . However, for a low-complexity

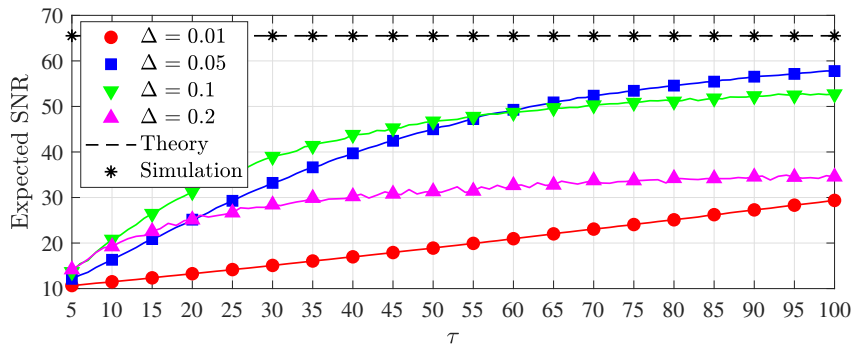


Fig. 2. Expected SNR versus duration of training period τ ; $P = 0$ dB, $\sigma^2 = 0$ dB.

scenario, τ is fixed and the maximum channel gain that can be achieved, highly depends on the choice of Δ . This is depicted in Fig. 2, where the expected SNR for the optimal beamforming gain $H^* = \left(\sum_{i=1}^M |h_i| |g_i|\right)^2$ is analytically given by

$$\begin{aligned}
\mathbb{E} \left\{ \frac{P}{\sigma^2} H^* \right\} &= \frac{P}{\sigma^2} \mathbb{E} \left\{ \sum_{i=1}^M |h_i|^2 |g_i|^2 + 2 \sum_{i=1}^{M-1} \sum_{j=i}^M |h_i| |g_i| |h_j| |g_j| \right\} \\
&\stackrel{(a)}{=} \frac{P}{\sigma^2} \left(M \mathbb{E} \{ |h|^2 |g|^2 \} + 2 \binom{M}{2} \mathbb{E} \{ |h| |g| \}^2 \right) \\
&\stackrel{(b)}{=} \frac{P}{\sigma^2} \left(2M \int_0^\infty x K_0(2\sqrt{x}) dx + 32 \binom{M}{2} \left(\int_0^\infty x^2 K_0(2x) dx \right)^2 \right) \\
&\stackrel{(c)}{=} \frac{P}{\sigma^2} \left(M + \binom{M}{2} \frac{\pi^2}{8} \right), \tag{22}
\end{aligned}$$

where (a) follows from the fact that $|h_i| |g_i|$ are mutually independent, (b) uses the PDFs $f_X(x) = 2K_0(2\sqrt{x})$ and $f_X(x) = 4xK_0(2x)$ of $|h|^2 |g|^2$ and $|h| |g|$, respectively [20], and (c) follows from [21, 6.561-16].

The outage probability achieved by the proposed algorithm can be written as

$$\Pi_{\text{OBF}}(\rho, \tau) = \mathbb{P} \left\{ \frac{1}{T} (R_{\text{TP}} + R_{\text{BF}}) < \rho \right\},$$

where

$$R_{\text{TP}} = \sum_{t=1}^{\tau} \log_2 \left(1 + \frac{P}{\sigma^2} H_t \right), \tag{23}$$

is the achieved sum-rate during the training period, and

$$R_{\text{BF}} = (T - \tau) \log_2 \left(1 + \frac{P}{\sigma^2} H_0 \right), \tag{24}$$

is the achieved sum-rate after completion of the training period, with constant phase rotations $\phi_{0,i}$ for $T - \tau$ channel uses; clearly, $\phi_{0,i} = \phi_{\tau,i}$ and $H_0 = H_\tau$. Furthermore, the energy efficiency achieved by the OBF scheme can be written as

$$\eta_{\text{OBF}} = \frac{1}{T} \frac{\sum_{t=1}^{\tau} \mathbb{E}\{\log_2(1 + \frac{P}{\sigma^2} H_t)\} + (T - \tau) \mathbb{E}\{\log_2(1 + \frac{P}{\sigma^2} H_0)\}}{P/\xi + P_S + P_D + P_{\text{IRS}}}, \quad (25)$$

where we assume that the power consumed by the one-bit feedback is negligible and so the total power consumption is equal to the one of the RRC scheme. In order to evaluate the expected rates in the above expression, we use the approximation of the expected rate for a channel with b feedback bits by [22]

$$\mathbb{E}\left\{\log_2\left(1 + \frac{P}{\sigma^2} H_t\right)\right\} \approx \mathbb{E}\left\{\log_2\left(1 + \frac{P}{\sigma^2} H^* \left(1 - 2^{-\frac{b}{M-1}}\right)\right)\right\}, \quad (26)$$

where the b feedback bits guarantee that each bit provides an increase in performance. However, based on the OBF scheme, not all feedback bits provide a performance gain. Hence, at the t -th time instant, we take $b = \kappa t$, $0 < \kappa \leq 1$, where κ defines the fraction of the t bits that resulted in a performance increase. In other words, κ determines the effectiveness of the algorithm. Therefore, from (26), we get

$$\begin{aligned} \mathbb{E}\left\{\log_2\left(1 + \frac{P}{\sigma^2} H^* \left(1 - 2^{-\frac{\kappa t}{M-1}}\right)\right)\right\} &\leq \log_2\left(1 + \frac{P}{\sigma^2} \mathbb{E}\{H^*\} \left(1 - 2^{-\frac{\kappa t}{M-1}}\right)\right) \\ &= \log_2\left(1 + \frac{P}{\sigma^2} \left(M + \binom{M}{2} \frac{\pi^2}{8}\right) \left(1 - 2^{-\frac{\kappa t}{M-1}}\right)\right), \end{aligned} \quad (27)$$

which follows from the Jensen's inequality and the result in (22). By substituting the above expression in (25), we get an approximation for the energy efficiency.

C. Diversity Analysis

The RRC scheme virtually behaves as an $T \times M$ Rayleigh product channel [23]. Since all the messages are sent by the source at each channel use, this is equivalent to using T antennas over one time slot. Additionally, due to the independent random phase rotations at the IRS, the scheme can achieve diversity order equal to $\min(T, M)$ [23]. By considering $P \rightarrow \infty$ and the two cases $M > T$ and $T < M$, we prove analytically in Appendix E that

$$d_{\text{RRC}} = \min(T, M), \quad (28)$$

and

$$G_{\text{RRC}} = \left(\frac{\sigma^2}{M}\right)^T (-1)^T \left(1 - 2^{\rho T} \sum_{t=0}^{T-1} \frac{(-1)^t}{t!} \log^t(2^{\rho T})\right), \quad (29)$$

is the achieved diversity order and array gain of the RRC scheme.

Finally, as the OBF scheme employs the RRC scheme for the first τ channel uses, we can deduce that its diversity order is also $\min(\tau, M)$.

V. SELECTION-BASED IRS SCHEMES

For the selection-based schemes, we consider $T = 1$ and assume that the IRS is partitioned into N non-overlapping sub-surfaces of m elements, where N is a divisor of M , i.e. $mN = M$. An example of the system model is illustrated in Fig. 1 with $N = 6$ and $m = 6$, where the partitions are shown by the solid lines. We consider a closed-loop system, that is, we assume there is knowledge of the received SNR power at the destination from each sub-surface via an error-free feedback scheme [26]. This can be implemented by a training period, where the received signal strength indicator (RSSI) is fed back to the IRS controller.

A. Transmit Diversity Scheme

For the TD scheme, the IRS controller selects and activates, at each time slot, the sub-surface which achieves the highest SNR at the destination. As a result, the destination needs to feed back to the IRS $b_{\text{TD}} = \lceil \log_2(N) \rceil$ bits. The outage probability achieved by the proposed TD scheme is given below.

Proposition 4. *The outage probability of the TD scheme is*

$$\Pi_{\text{TD}}(\rho) = \Pi(\rho, 1)^N, \quad (30)$$

where N is the number of sub-surfaces with m elements and $\Pi(\rho, 1)$ is the outage probability of a random selection given by Proposition 1 with $M = m$.

Proof. Assume the ordering

$$\gamma_{(1)} \geq \gamma_{(2)} \geq \dots \geq \gamma_{(N)}, \quad (31)$$

where $\gamma_{(i)}$, $1 \leq i \leq N$, is the i -th highest receiver SNR at the destination from the N sub-surfaces of the IRS. Then, using the distribution of ordered random variables, the outage probability is [26]

$$\Pi_{\text{TD}}(\rho) = \mathbb{P}\{\log_2(1 + \gamma) < \rho\}^N, \quad (32)$$

where $\mathbb{P}\{\log_2(1 + \gamma) < \rho\}$ is the outage probability when $T = 1$ given by Proposition 1 and the result follows. \square

For the sake of completeness, we also provide the outage probability for the TD scheme with coherent transmissions.

Corollary 1. *The outage probability of the TD scheme with coherent transmissions is given by $\Pi_{\text{TDCT}}(\rho) = \Pi_{\text{CT}}(\rho)^N$, where $\Pi_{\text{CT}}(\rho)$ is given by Proposition 2 with $M = m$.*

The proof is omitted as it follows the same steps as the one of Proposition 4. In what follows, we evaluate the energy efficiency of the TD scheme.

Proposition 5. *The expected rate achieved by the TD scheme is*

$$R_{\text{TD}} = N \int_0^\infty \log_2 \left(1 + \frac{P}{\sigma^2} h \right) F_H(h)^{N-1} f_H(h) dh, \quad (33)$$

where $f_H(h)$ and $F_H(h)$ are given by (14) and (50), respectively.

Proof. See Appendix F. \square

Therefore, the energy efficiency achieved by the TD scheme is

$$\eta_{\text{TD}} = \frac{R_{\text{TD}}}{P/\xi + P_S + P_D + P_{\text{IRS}}}, \quad (34)$$

where the power consumption parameters are defined as before but with $P_{\text{IRS}} = mP_E$, since only m elements are activated at each time slot. It is clear, that $\eta_{\text{TD}} = \eta_{\text{RRC}}$ when $N = T = 1$. However, for $N = T > 1$, the denominator of (34) is always less than the one of (18), since $m < M$. Hence, due to the selection process, the selection-based scheme TD will have higher energy efficiency at the high SNR regime.

Note that for $N = 1$, Proposition 5 provides the expected rate for a randomly selected sub-surface. Moreover, the expected rate achieved by the TD scheme with coherent transmissions can be evaluated by $R_{\text{TDCT}} = \int_0^\infty (1 - \Pi_{\text{TDCT}}(\rho)) d\rho$. Then, the energy efficiency can be computed accordingly by (34), where the power consumption is equal to the non-coherent case.

B. Adaptive Transmit Diversity Scheme

We now consider the ATD scheme, where the IRS selects a sub-surface which achieves an SNR at the destination of at least ψ [29]. Initially, the IRS activates a random sub-surface and the destination feeds back one bit, representing whether or not the received signal achieved the

threshold ψ . In case of a positive feedback, the IRS selects that sub-surface for the remaining communication period; otherwise, the same process is repeated with a different sub-surface. If the first $N - 1$ sub-surfaces do not satisfy the selection criterion, then the IRS selects the N -th sub-surface, regardless of its achieved SNR.

Without loss of generality, assume that the IRS activates the sub-surfaces in an order which achieve SNRs $\gamma_1, \gamma_2, \dots, \gamma_{N-1}$. Therefore, the average number of feedback bits needed are

$$b_{\text{ATD}} = 1 + \sum_{i=1}^{N-2} \mathbb{P}\{\log_2(1 + \gamma_i) < \psi\} = 1 + (N - 2)\Pi(\psi, 1), \quad (35)$$

where $\Pi(\psi, 1)$ is given by Proposition 1. The outage probability for this scheme, is given by the following proposition.

Proposition 6. *The outage probability of the ATD scheme is*

$$\Pi_{\text{ATD}}(\rho, \psi) = \Pi(\psi, 1)^{N-1}\Pi(\rho, 1) + \mathbf{1}_{\rho > \psi}(\Pi(\rho, 1) - \Pi(\psi, 1)) \sum_{k=0}^{N-2} \Pi(\psi, 1)^k, \quad (36)$$

where N is the number of sub-surfaces with m elements and $\Pi(\rho, 1)$ is the outage probability of a random selection given by Proposition 1 with $M = m$.

Proof. See Appendix G. □

We can observe from Proposition 6, that an increase in N is always beneficial for the case $\rho \leq \psi$. However, when $\rho > \psi$, the second term in (36) increases with N . In addition, the case $\psi = \rho$, describes the TD scheme. Now, for the expected rate of this scheme, we can write

$$\begin{aligned} R_{\text{ATD}} &= \sum_{k=0}^{N-2} \Pi(\psi, 1)^k \int_{\psi}^{\infty} \log_2 \left(1 + \frac{P}{\sigma^2} h \right) f_H(h) dh \\ &\quad + \Pi(\psi, 1)^{N-1} \int_0^{\infty} \log_2 \left(1 + \frac{P}{\sigma^2} h \right) f_H(h) dh, \end{aligned} \quad (37)$$

where $f_H(h)$ is given by (14). We omit the proof for brevity as it follows a similar approach as the proof of Proposition 3.

Note that this scheme could be generalized, in the sense that the IRS could stop after activating K sub-surfaces, with $K \leq N - 1$. The considered case provides the upper bound in terms of performance, but our analysis could be generalized by simply setting $N = K + 1$. Finally, the energy efficiency η_{ATD} of the ATD scheme is simply given by (34) but with expected rate R_{ATD} provided above.

C. Diversity Analysis

We now derive the diversity order and array gain of the selection-based schemes; the proofs can be found in Appendix H. Specifically, the TD scheme, achieves full spatial diversity order, i.e., $d_{\text{TD}} = N$, as expected. Moreover, its achieved array gain is equal to

$$G_{\text{TD}} = \left(\frac{\sigma^2}{m}\right)^N (2^\rho - 1)^N \leq G_{\text{RRC}}, \quad (38)$$

where the inequality is valid for $N = T$ and $m = M$, by comparing the non-common factor of the two expressions. In this case, the selection-based TD scheme can provide better array gains compared to the RRC scheme.

The diversity order of the coherent TD case is $d_{\text{TDCT}} = mN$, as expected, and the array gain of this scheme is

$$G_{\text{TDCT}} = \left((-1)^{m+1} \frac{(\theta\sigma^2)^m}{\pi(2m)!} \int_0^\infty \Im(\phi_H(t)) t^{2m-1} dt \right)^N. \quad (39)$$

Finally, the diversity order of the ATD scheme depends on whether or not $\rho \leq \psi$. In particular, if $\rho \leq \psi$, it is clear from Proposition 6 that the diversity order is N with an array gain

$$G_{\text{ATD}} = \left(\frac{\sigma^2}{m}\right)^N (2^\psi - 1)^{N-1} (2^\rho - 1) \geq G_{\text{TD}}, \quad (40)$$

where equality holds for $\psi = \rho$. On the other hand, if $\rho > \psi$, the second term of (36) dominates and so the achieved diversity is one.

D. Limiting Distribution

Next, we consider the asymptotic behavior of the TD scheme as N increases. Clearly, when $N \rightarrow \infty$ then $M \rightarrow \infty$, which corresponds to a massive multiple-element configuration and is a case of practical interest [2], [6].

Now, based on extreme value theory, when the selection is done over a large number of sub-surfaces, the limiting distribution of the largest order statistic can be one of three domains of attraction, namely, the Fréchet, the Weibull and the Gumbel distribution [26]. In our case, using Lemma 1, we can easily prove that the parent distribution satisfies

$$\lim_{x \rightarrow \infty} \frac{1 - F_H(x)}{f_H(x)} = c, \quad (41)$$

where $c > 0$ is a constant. As a result, $\Pi_{\text{TD}}(\rho)$ converges to a Gumbel distribution, i.e.,

$$\Pi_{\text{TD}}(\rho) = G\left(\frac{\theta\sigma^2/P - b_N}{a_N}\right), \quad (42)$$

TABLE I
THE PROPOSED IRS SCHEMES

Scheme	Description	Diversity	# of feedback bits
RRC	Coding through random rotations achieves artificial fast fading channel	$\min(T, M)$	0
OBF	Coding through one-bit feedback to achieve beamforming	$\min(\tau, M)$	τ
TD	Sub-surface selection based on highest SNR at destination	N	$\lceil \log_2(N) \rceil$
ATD	Sub-surface selection based on pre-defined SNR threshold at destination	N if $\rho \leq \psi$, 1 if $\rho > \psi$	$1 + (N - 2)\Pi(\psi, 1)$

where $G(x)$ is given by

$$G(x) = \exp(-\exp(-x)), \infty < x < \infty. \quad (43)$$

Moreover, a_N and b_N are normalizing constants satisfying the following condition

$$\lim_{N \rightarrow \infty} F_H(a_N x + b_N) = G(x), \quad (44)$$

where $F_H(\cdot)$ is given by Lemma 1. These constants can be computed by solving the following

$$1 - F_H(b_N) = \frac{1}{m}, \quad (45)$$

and

$$1 - F_H(a_N + b_N) = \frac{1}{em}, \quad (46)$$

where e is Euler's number, which results in $a_N = m$ and $b_N = m \log(N)$. Therefore, we have

$$\Pi_{\text{TD}}(\rho) = \exp\left(-\exp\left(-\frac{\theta\sigma^2/P - m \log(N)}{m}\right)\right) = \exp\left(-N \exp\left(-\frac{\theta\sigma^2}{Pm}\right)\right). \quad (47)$$

VI. DISCUSSION & NUMERICAL RESULTS

A brief discussion is provided to highlight the benefits and capabilities of the proposed IRS schemes; Table I summarizes their main characteristics. Firstly, it is important to point out, that a coding-based scheme can easily be jointly implemented with a selection-based scheme. For example, the RRC scheme could be employed with the TD scheme on the selected sub-surface. In this paper, we consider them separately so as to emphasize the benefits of each approach and their joint consideration is a simple extension of the derived analytical results. Secondly,

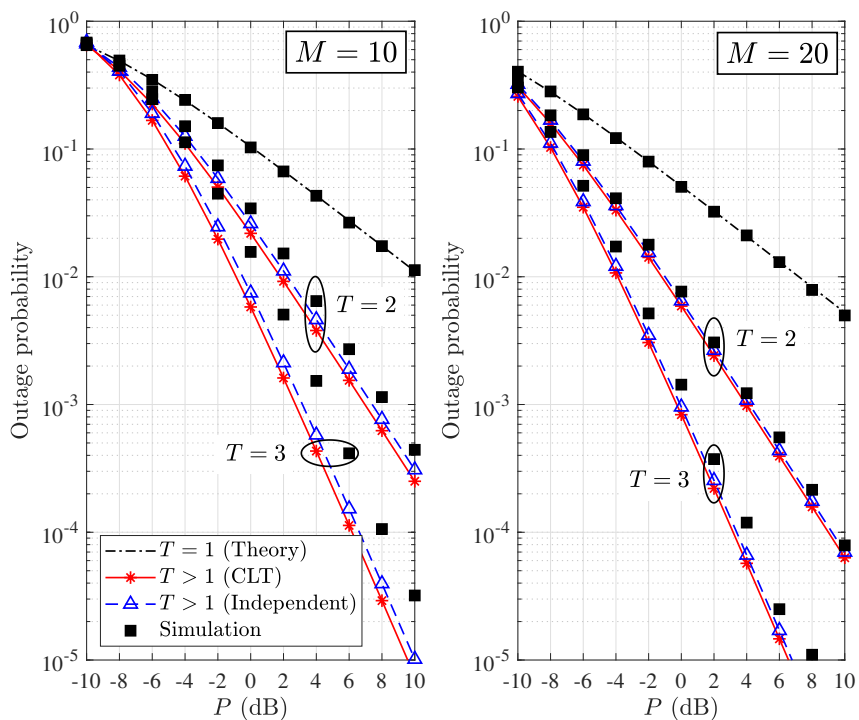


Fig. 3. Outage probability versus P for the RRC scheme.

all schemes can achieve full diversity with a low-complexity feedback protocol, requiring only a small number of bits for their implementation (see Table I). Note that the RRC scheme does not require any feedback from the destination and ATD scheme needs only 1 bit at the high SNR regime (since $P \rightarrow \infty$ implies $\Pi(\psi, 1) \rightarrow 0$). In addition, the random rotation of the phases at each IRS element guarantees that the complexity at the IRS is kept low, independently of the phases' resolution. Finally, all schemes provide good performances in terms of outage probability, rate and energy efficiency, which is evident from the numerical results below.

We now validate our theoretical analysis and main analytical assumptions with computer simulations and show the benefits of our proposed schemes. For the sake of presentation, we consider $\rho = 1$ bps/Hz, $\sigma^2 = 0$ dB, $\xi = 1.2$, $P_E = 10$ dBm, $P_D = 10$ dBm and $P_S = 9$ dBW [12]. Unless otherwise stated, lines correspond to theoretical results whereas markers correspond to simulation results.

Fig. 3 depicts the outage probability achieved by the RRC scheme in terms of the transmit power P , the number of channel uses T and the number of reflecting elements M . As expected, the performance is improved with an increase of M . Moreover, and most importantly, increasing the number of channel uses T provides significant gains to the outage probability. It should be

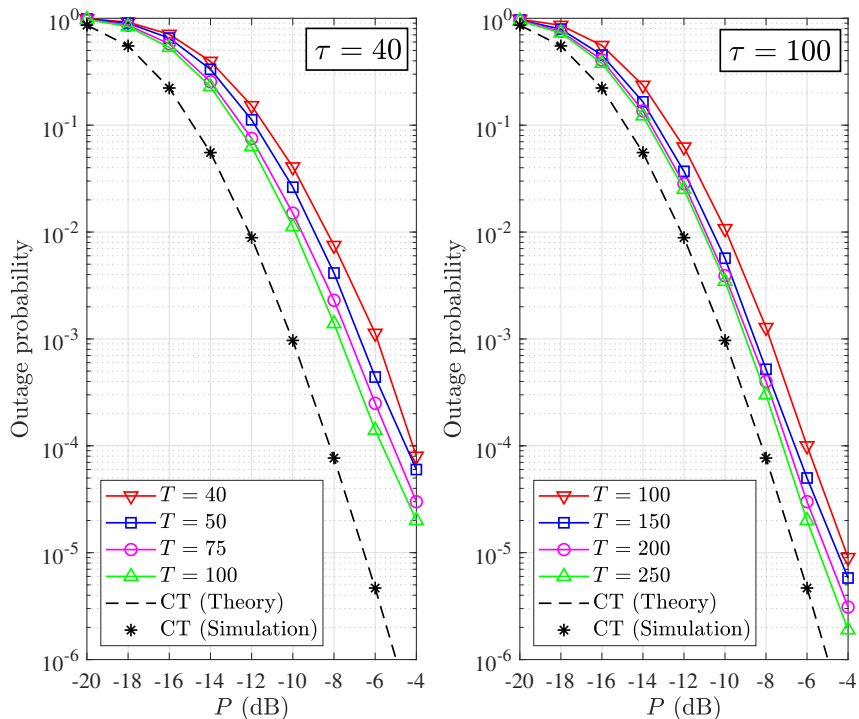


Fig. 4. Outage probability versus P for the OBF scheme; $M = 10$.

highlighted that the massive benefits of this scheme are evident from $T = 2$, which is the smallest number of channel uses the scheme can employ. Also, we can observe that the scheme provides full diversity order T , since $T < M$, as deduced by our analysis. Finally, the figure validates the considered assumptions and approximations of our theoretical study. Specifically, for $T = 1$, the simulation results perfectly match the theoretical result of Proposition 1. Furthermore, for $T > 1$, the expressions of Theorem 1 and Theorem 2, approximate the achieved outage probability exceptionally well even for small M and the approximations become tighter as M increases.

Fig. 4 shows the achieved outage probability of the OBF scheme with $M = 10$ and for the cases $\tau = 40$ with $\delta = 0.1$ and $\tau = 100$ with $\delta = 0.05$. The performance of the OBF scheme is compared to the coherent (beamforming) case which is the best scenario that can be achieved; the theoretical and simulation results for the coherent case agree, which verifies our analysis. It is clear that as τ increases, the OBF gets closer to the beamforming case, as also shown in Section IV-B with Fig. 2. However, for a fixed τ , the outage probability converges to a lower bound as T increases. Thus, for a low-complexity scenario, T does not need to be much larger than τ .

Fig. 5 illustrates the performance of the selection-based TD scheme with regards to the number

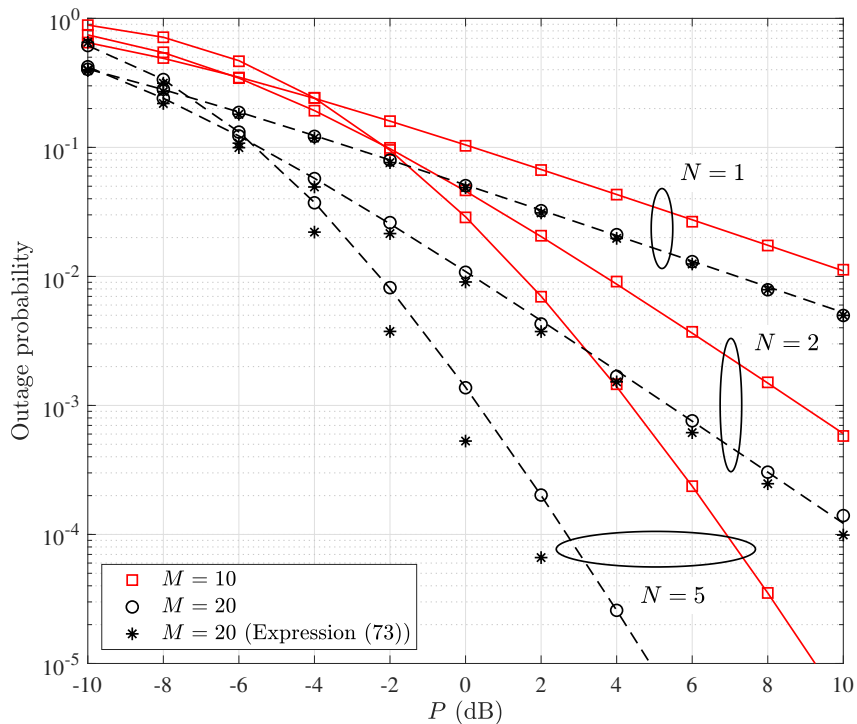


Fig. 5. Outage probability versus P for the TD scheme.

of reflecting elements M and the number of sub-surfaces N . Again, the theoretical and simulation results are in agreement, which validates our analysis. In addition, we show the approximation of the TD scheme, given by (73). We can see that the approximation follows the behavior of the curves very well and it matches the simulation for high values of M ($N = 1$), which validates the consideration of Lemma 1. It is clear that the selection process improves the performance as N increases, especially in the high SNR regime, where the scheme achieves full spatial diversity order. We should emphasize here that for $M = 20$ and $N = 5$, only four passive elements reflect their incident signal compared to the case $N = 1$, for which there are twenty active elements. This shows how this scheme is energy efficient and of low-complexity but still provides performance gains.

Fig. 6 depicts the outage probability for the selection-based schemes, in terms of the number of sub-surfaces N . In contrast to the other cases, the performance of the ATD scheme with $\psi = 0.9$, diminishes as N increases. Since $\psi = 0.9 < \rho$, the IRS could select a sub-surface with achieved SNR greater than ψ but lower than ρ . As N increases, this selection is more likely and so the outage probability increases as well. On the other hand, when $\psi = 1.1 > \rho$, the outage probability decreases with N , since a selection in this case implies that the destination will not be

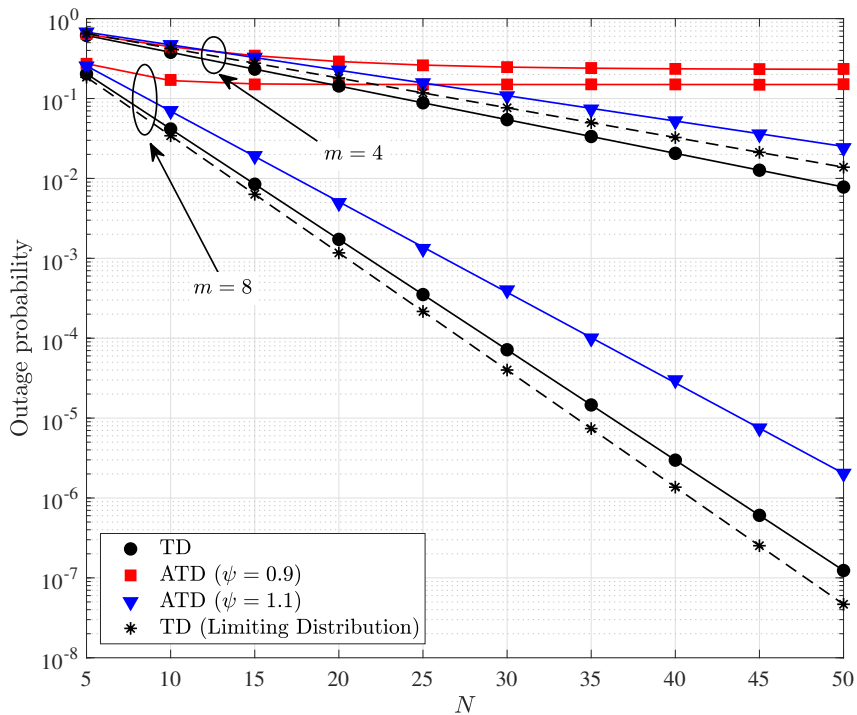


Fig. 6. Outage probability versus N for the selection-based schemes; $P = -10$ dB.

in outage. These observations can also be derived from the analytical expression in Proposition 6. It is important to note that, even though the TD scheme outperforms the ATD scheme, its implementation may require more bits of feedback. Fig. 6 also shows the performance of TD using the limiting distribution. Despite deriving the limiting distribution using Lemma 1, we can see that it still describes the system's behavior very well.

Finally, Fig. 7 shows the energy efficiency of the proposed schemes for different values of M and for $P = -10$ dB (left sub-figure) and $P = 0$ dB (right sub-figure). The first main observation, is that the energy efficiency initially increases with M but, after a certain value of M , it starts to decrease. This is expected, since the rate grows logarithmically but the power consumption grows linearly with M . Secondly, the energy efficiency of the RRC scheme is the same as with the conventional case ($T = 1$). As shown in Section IV-A, on average the rates of the two scenarios are equal. The OBF scheme outperforms all other schemes since at each time instant, the destination experiences a higher channel gain and gets closer to the beamforming gain. It is important to note here that our analytical approach to the OBF scheme provides a close approximation. The TD scheme has a smaller energy efficiency for small values of M , compared to the other two cases. However, as M increases, the TD scheme becomes more energy efficient

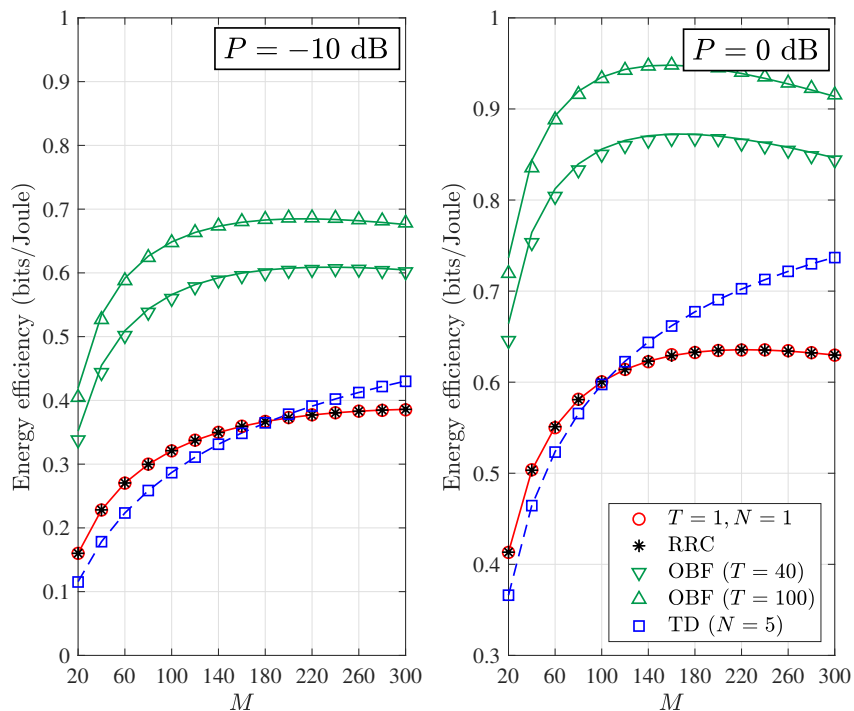


Fig. 7. Energy efficiency versus number of elements M ; $\tau = 40$, $\kappa = 0.5$, $\Delta = 0.1$.

due to the fact that it activates a fraction of the available elements at the IRS. Therefore, the energy efficiency of the TD scheme will start to decrease at larger values of M compared to the other schemes; this is clearly more evident for the case $P = 0$ dB.

VII. CONCLUSION

In this paper, we focused on an analytical framework for random rotation-based IRS-aided communications and presented four low-complexity and energy efficient schemes. In particular, we proposed two coding-based schemes, which produce a time-varying channel through time-varying random rotations. Moreover, we proposed two selection-based schemes, which activate a partition of the IRS elements based on received signal power at the destination. Analytical expressions were derived for the outage probability and energy efficiency of all the proposed schemes. Moreover, the diversity order together with the array gain achieved by each scheme was provided. Our results demonstrated that the proposed schemes provide significant performance gains compared to the conventional case, whilst keeping the complexity low and the energy efficiency high.

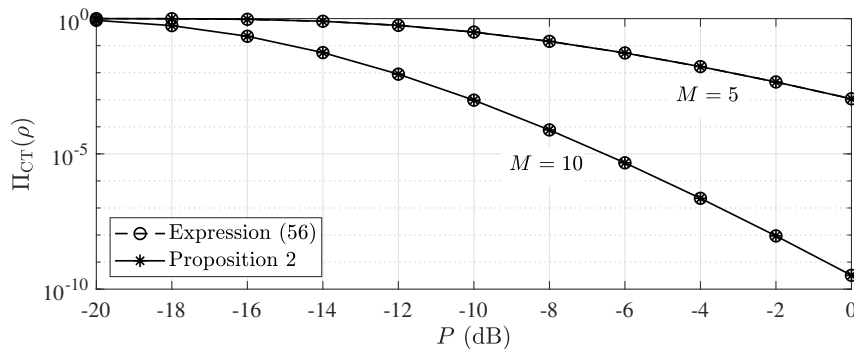


Fig. 8. $\Pi_{CT}(\rho)$ versus P with $\theta = 1$, $\sigma^2 = 0$ dB; even though Proposition 2 ignores the first $2m - 1$ terms of the sum in expression (56), both provide the same result which validates our approach.

APPENDIX A

PROOF OF PROPOSITION 1

Note that, due to the random rotations and since $T = 1$, the channel gain from the M elements of the IRS is

$$H_1 = \left| \sum_{i=1}^M h_i g_i \exp(j\phi_{1,i}) \right|^2 = \left| \sum_{i=1}^M h_i g_i \right|^2, \quad (48)$$

that is, the phases have no effect on the channel gain. Then, the outage probability when $T = 1$ can be evaluated as follows

$$\begin{aligned} \Pi(\rho, 1) &= \mathbb{P}\{\log_2(1 + \gamma_1) < \rho\} \\ &= \mathbb{P}\left\{ \frac{P}{\sigma^2} H_1 < 2^\rho - 1 \right\} \\ &= \mathbb{P}\left\{ \left| \sum_{i=1}^M h_i g_i \right|^2 < \frac{\theta \sigma^2}{P} \right\}, \end{aligned} \quad (49)$$

where $\theta \triangleq 2^\rho - 1$. The final expression is then derived by using

$$F_{H_1}(x) = 1 - \frac{2x^{M/2} K_M(2\sqrt{x})}{\Gamma(M)}, \quad (50)$$

which is the cumulative distribution function (CDF) of H_1 [27].

APPENDIX B

PROOF OF PROPOSITION 2

In the case of coherent transmission, the channel gain is given by

$$H = \left(\sum_{i=1}^M |h_i| |g_i| \right)^2. \quad (51)$$

Then, the outage probability can be evaluated as

$$\begin{aligned}\Pi_{\text{CT}}(\rho) &= \mathbb{P} \left\{ \left(\sum_{i=1}^M |h_i| |g_i| \right)^2 < \frac{\theta \sigma^2}{P} \right\} \\ &= \mathbb{P} \left\{ \sum_{i=1}^M |h_i| |g_i| < \sqrt{\frac{\theta \sigma^2}{P}} \right\}.\end{aligned}\quad (52)$$

Now, the PDF for the product of two Rayleigh random variables $|h|$ and $|g|$ is [27]

$$f_{|h||g|}(x) = 4xK_0(2x). \quad (53)$$

By using the above PDF, the characteristic function $\phi_{|h||g|}(t)$ of $|h||g|$ can be evaluated as

$$\begin{aligned}\phi_{|h||g|}(t) &= \mathbb{E}_{|h||g|} \{ \exp(jt|h||g|) \} \\ &= 4 \int_0^\infty \exp(jtx) x K_0(2x) dx \\ &= \frac{4\sqrt{t^2+4} + 2j\pi t - 4t \sinh^{-1}\left(\frac{t}{2}\right)}{(t^2+4)^{3/2}},\end{aligned}\quad (54)$$

which follows with the help of [21, 6.624-1] and the fact that $\log(j) = j\pi/2$ and $\log(t + \sqrt{t^2+1}) = \sinh^{-1}(t)$ [21], where $\sinh(\cdot)$ is the hyperbolic sine function. Using the Gil-Pelaez inversion theorem [28], we can obtain $\Pi_{\text{CT}}(\rho)$ as follows

$$\Pi_{\text{CT}}(\rho) = \frac{1}{2} - \frac{1}{\pi} \int_0^\infty \frac{1}{t} \Im \left(\exp \left(-jt \sqrt{\frac{\theta \sigma^2}{P}} \right) \phi_H(t) \right) dt, \quad (55)$$

where $\phi_H(t)$ is the characteristic function of H . Since H is the sum of M independent products of Rayleigh random variables, its characteristic function is $\phi_H(t) = \phi_{|h||g|}(t)^M$, where $\phi_{|h||g|}(t)$ is given by (54). By applying a Taylor series expansion to the exponential function in (55) and using the fact that $\int_0^\infty \frac{1}{t} \Im(\phi_H(t)) dt = \pi/2$, we have

$$\Pi_{\text{CT}}(\rho) = -\frac{1}{\pi} \int_0^\infty \frac{1}{t} \Im \left(\sum_{i=1}^\infty \left(-jt \sqrt{\frac{\theta \sigma^2}{P}} \right)^i \frac{1}{i!} \phi_H(t) \right) dt. \quad (56)$$

The final result follows by taking into account that the first $2m-1$ terms of the above sum are zero; this is validated by Fig. 8.

APPENDIX C

PROOF OF LEMMA 1

Let $W_t = \sum_{i=1}^M h_i g_i \exp(j\phi_{t,i})$. Then, W_t can be expressed as $W_t = X_t + jY_t$, where

$$X_t = \sum_{i=1}^M |h_i| |g_i| \cos(\phi_{t,i} + \chi_i + \psi_i), \quad (57)$$

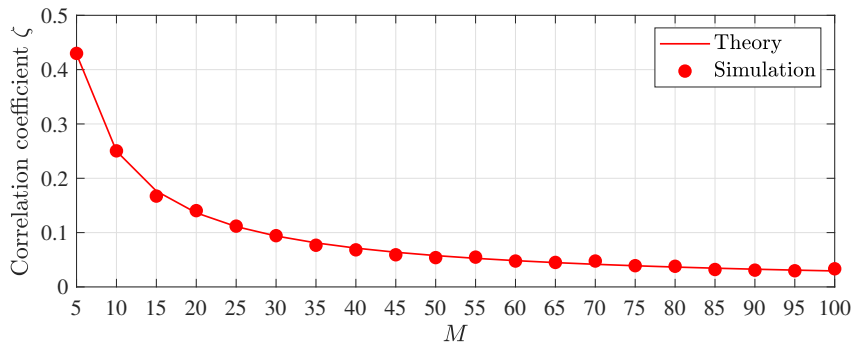


Fig. 9. Correlation coefficient ζ versus M .

and

$$Y_t = j \sum_{i=1}^M |h_i| |g_i| \sin(\phi_{t,i} + \chi_i + \psi_i). \quad (58)$$

As $h_i \sim \mathcal{CN}(0, 1)$ and $g_i \sim \mathcal{CN}(0, 1)$, implies that $\mathbb{E}\{|h_i|\} = \mathbb{E}\{|g_i|\} = \sqrt{\frac{\pi}{2}}$ and $\mathbb{E}\{\cos(\phi_{t,i} + \chi_i + \psi_i)\} = \mathbb{E}\{\sin(\phi_{t,i} + \chi_i + \psi_i)\} = 0$. Therefore, the mean of each summand is simply $\mathbb{E}\{|h_i| |g_i| \cos(\phi_{t,i} + \chi_i + \psi_i)\} = \mathbb{E}\{|h_i| |g_i| \sin(\phi_{t,i} + \chi_i + \psi_i)\} = 0$. Moreover, the variance of each summand is given by $\mathbb{E}\{|h_i|^2 |g_i|^2 \cos^2(\phi_{t,i} + \chi_i + \psi_i)\} = \mathbb{E}\{|h_i|^2 |g_i|^2 \sin^2(\phi_{t,i} + \chi_i + \psi_i)\} = 1/2$ since $\mathbb{E}\{|h_i|^2\} = \mathbb{E}\{|g_i|^2\} = 1$ and $\mathbb{E}\{\cos^2(\phi_{t,i} + \chi_i + \psi_i)\} = \mathbb{E}\{\sin^2(\phi_{t,i} + \chi_i + \psi_i)\} = 1/2$.

Thus, by applying the CLT, we have that X_t and Y_t are Gaussian random variables with mean $\mu_{X_t} = \mu_{Y_t} = 0$ and variance $\sigma_{X_t}^2 = \sigma_{Y_t}^2 = M/2$. As such, W_t converges in distribution to a complex Gaussian random variable. Therefore, $H_t = |W_t|^2$ is exponentially distributed with parameter $1/M$.

APPENDIX D

PROOF OF THEOREM 1

The random variables $H_t = \left| \sum_{i=1}^M h_i g_i \exp(j\phi_{t,i}) \right|^2$ are correlated since the channel coefficients h_i and g_i remain constant over all T transmissions. However, as M increases, the correlation between the random variables H_t decreases. In particular, the correlation coefficient ζ between H_{t_1} and H_{t_2} , $t_1 \neq t_2$, is given by

$$\zeta = \frac{\mathbb{E}\{H_{t_1} H_{t_2}\} - \mathbb{E}\{H_{t_1}\} \mathbb{E}\{H_{t_2}\}}{\sigma_{H_{t_1}} \sigma_{H_{t_2}}} = \frac{3}{M+2}, \quad (59)$$

where $\sigma_{H_i} = \sqrt{\mathbb{E}\{H_i^2\} - \mathbb{E}\{H_i\}^2}$, $\mathbb{E}\{H_i\} = M$, $\mathbb{E}\{H_i^2\} = 2M(M+1)$ and $\mathbb{E}\{H_i H_j\} = M(M+3)$. It is clear that for $M \rightarrow \infty$ we have $\zeta \rightarrow 0$; this is also depicted in Fig. 5. By taking this into consideration, we can evaluate the outage probability as follows

$$\begin{aligned} \Pi_{\text{RRC}}^{\text{IND}}(\rho, T) &= \mathbb{P} \left\{ \frac{1}{T} \sum_{t=1}^T \log_2(1 + \gamma_t) < \rho \right\} \\ &= \mathbb{P} \left\{ \log_2 \prod_{t=1}^T (1 + \gamma_t) < T\rho \right\} \\ &= \mathbb{E}_{H_k} \left\{ F_{H_1} \left(\frac{\sigma^2}{P} \left(\frac{2^{T\rho}}{\prod_{t=2}^T (1 + PH_t/\sigma^2)} - 1 \right) \right) \right\}, \end{aligned} \quad (60)$$

which follows by the logarithmic identity $\log_2(x) + \log_2(y) = \log_2(xy)$, solving for H_1 and using the CDF of H_1 given by (50). Since the random variables H_t are assumed to be independent, we have

$$\begin{aligned} \Pi_{\text{RRC}}^{\text{IND}}(\rho, T) &= \int_{z_T} \cdots \int_{z_2} F_{H_1} \left(\frac{\sigma^2}{P} \left(\frac{2^{T\rho}}{\prod_{t=2}^T (1 + Pz_t/\sigma^2)} - 1 \right) \right) \\ &\quad \times \prod_{t=2}^T f_{H_t}(z_t) dz_2 \cdots dz_T, \end{aligned} \quad (61)$$

where $f_{H_t}(z_t)$ is the PDF of H_t given by the derivative of (50). The integration limits are evaluated by considering the inequality

$$\frac{2^{T\rho}}{\prod_{t=2}^T (1 + Pz_t/\sigma^2)} - 1 > 0, \quad (62)$$

sequentially for each z_t . Finally, the transformation $w_t \rightarrow 1 + Pz_t/\sigma^2$ provides the final expression.

APPENDIX E

DIVERSITY OF RRC SCHEME

Firstly, assume that $M > T$. Then, we can use Theorems 1 and 2 to derive the diversity order. By employing the approximation $K_M(x) \approx \Gamma(M)2^{M-1}/x^M$ for $x \approx 0$ [21] in Theorem 1, we can see that the outage probability $\Pi_{\text{RRC}}^{\text{IND}}(\rho, T)$ reduces to zero. This is because the convergence to the diversity order for cascaded channels is very slow and is observed for very high SNR values [24]. However, using the approximated expression in Theorem 2 and the fact that $\exp(-x) \approx 1 - x$ for $x \approx 0$, we have

$$\lim_{P \rightarrow \infty} \Pi_{\text{RRC}}^{\text{CLT}}(\rho, T) \approx \left(\frac{\sigma^2}{MP} \right)^T \int_1^{\xi_T} \cdots \int_1^{\xi_2} \left(\frac{2^{\rho T}}{\prod_{t=2}^T w_t} - 1 \right)$$

$$\times \prod_{t=2}^T \left(1 - \frac{\sigma^2}{MP}(w_t - 1)\right) dw_2 \cdots dw_T \quad (63)$$

$$\rightarrow O(1/P^T),$$

where it is clear that the expansion of the second product in (63), will be a sum of 2^{T-1} terms, out of which only the term equal to one will not contain $1/P$. Therefore, as the smallest order term will dominate the others, it follows that the RRC scheme achieves time diversity of order T with array gain G_{RRC} equal to

$$\begin{aligned} G_{\text{RRC}} &= \left(\frac{\sigma^2}{M}\right)^T \int_1^{\xi_T} \cdots \int_1^{\xi_2} \left(\frac{2^{\rho T}}{\prod_{t=2}^T w_t} - 1\right) dw_2 \cdots dw_T \\ &= \left(\frac{\sigma^2}{M}\right)^T (-1)^T \left(1 - 2^{\rho T} \sum_{t=0}^{T-1} \frac{(-1)^t}{t!} \log^t(2^{\rho T})\right), \end{aligned} \quad (64)$$

which follows by evaluating the $(T-1)$ -fold integral and after some trivial algebraic manipulations.

Now, consider the case $T > M$. In fact, assume that $T \rightarrow \infty$. In this case, we have

$$\lim_{T \rightarrow \infty} \frac{1}{T} \sum_{t=1}^T \log_2(1 + \gamma_t) = \mathbb{E}_\phi \left\{ \log_2 \left(1 + \frac{P}{\sigma^2} \left| \sum_{i=1}^M h_i g_i \exp(j\phi_i) \right|^2 \right) \right\}, \quad (65)$$

where $\phi = [\phi_1 \ \phi_2 \ \cdots \ \phi_M]$. Moreover, at the high SNR regime, we have [25]

$$\mathbb{P} \left\{ \mathbb{E}_\phi \left\{ \log_2 \left(1 + \frac{P}{\sigma^2} \left| \sum_{i=1}^M h_i g_i \exp(j\phi_i) \right|^2 \right) \right\} < \rho \right\} \doteq \mathbb{P} \left\{ \log_2 \left(1 + \frac{P}{\sigma^2} \sum_{i=1}^M |h_i|^2 |g_i|^2\right) < \rho \right\}, \quad (66)$$

where the relation $\alpha \doteq \beta^c$ means $\lim_{\beta \rightarrow 0} \frac{\log \alpha}{\log \beta} = c$ [25]. Hence, this implies that we can use $\mathbb{P} \left\{ \log_2 \left(1 + \frac{P}{\sigma^2} \sum_{i=1}^M |h_i|^2 |g_i|^2\right) < \rho \right\}$ to derive the scheme's diversity order. By following a similar approach as in Proposition 2, we have

$$\mathbb{P} \left\{ \sum_{i=1}^M |h_i|^2 |g_i|^2 < (2^\rho - 1) \frac{\sigma^2}{P} \right\} = \frac{1}{\pi} \int_0^\infty \Im \left(\phi(t) \sum_{i=M}^\infty (-1)^{i+1} \left(j \frac{\theta \sigma^2}{P} \right)^i \frac{t^{i-1}}{i!} \right) dt, \quad (67)$$

with $\theta = 2^\rho - 1$ and $\phi(t) = \left(\int_0^\infty \exp(jth) f(h) dh \right)^M$, where $f(h) = 2K_0(2\sqrt{h})$ is the PDF of $|h|^2 |g|^2$. Then, for $P \rightarrow \infty$, we have

$$\begin{aligned} &\lim_{P \rightarrow \infty} \frac{1}{\pi} \int_0^\infty \Im \left(\phi(t) \sum_{i=M}^\infty (-1)^{i+1} \left(j \frac{\theta \sigma^2}{P} \right)^i \frac{t^{i-1}}{i!} \right) dt \\ &\approx \frac{1}{\pi} \int_0^\infty \Im \left(\phi(t) (-1)^{M+1} \left(j \frac{\theta \sigma^2}{P} \right)^M \frac{t^{M-1}}{M!} \right) dt \rightarrow O(1/P^M), \end{aligned} \quad (68)$$

which shows that the diversity order is M .

APPENDIX F

PROOF OF PROPOSITION 5

Given the SNR ordering $\gamma_{(1)} \geq \gamma_{(2)} \geq \dots \geq \gamma_{(N)}$, the expected rate of the highest received SNR $\gamma_{(1)}$ at the destination can be derived as

$$\begin{aligned} \mathbb{E}_{\gamma_{(1)}} \{\log_2(1 + \gamma_{(1)})\} &= \mathbb{E}_{H_{(1)}} \left\{ \log_2 \left(1 + \frac{P}{\sigma^2} H_{(1)} \right) \right\} \\ &= \int_0^\infty \log_2 \left(1 + \frac{P}{\sigma^2} h \right) p_{H_{(1)}}(h) dh, \end{aligned} \quad (69)$$

where $p_{H_{(1)}}$ is the probability distribution function (PDF) of the largest order statistic $H_{(1)}$ given by [26]

$$p_{H_{(1)}}(h) = N F_H(h)^{N-1} f_H(h). \quad (70)$$

By replacing the above PDF in (69), completes the proof.

APPENDIX G

PROOF OF PROPOSITION 6

Two cases need to be considered, namely, $\rho \leq \psi$ and $\rho > \psi$. The former case implies that outage could occur, in the event of $N - 1$ sub-surfaces not satisfying the selection criterion. As the events are mutually exclusive, we have

$$\Pi_{\text{ATD}}(\rho, \psi \mid \rho \leq \psi) = \mathbb{P}\{\log_2(1 + \gamma_1) < \psi\} \cdots \mathbb{P}\{\log_2(1 + \gamma_{N-1}) < \psi\} \mathbb{P}(\log_2(1 + \gamma_N) < \rho). \quad (71)$$

In the other case, outage could occurs when the i -th sub-surface, $1 \leq i \leq N - 1$, satisfies the selection criterion but not the outage threshold or when $N - 1$ sub-surfaces are not selected and the N -th is in outage. In mathematical terms,

$$\begin{aligned} \Pi_{\text{ATD}}(\rho, \psi \mid \rho > \psi) &= \mathbb{P}\{\psi < \log_2(1 + \gamma_1) < \rho\} + \mathbb{P}\{\log_2(1 + \gamma_1) < \psi\} \mathbb{P}\{\psi < \log_2(1 + \gamma_2) < \rho\} \\ &\quad + \cdots + \mathbb{P}\{\log_2(1 + \gamma_1) < \psi\} \cdots \mathbb{P}\{\log_2(1 + \gamma_{N-2}) < \psi\} \mathbb{P}\{\psi < \log_2(1 + \gamma_{N-1}) < \rho\} \\ &\quad + \mathbb{P}\{\log_2(1 + \gamma_1) < \psi\} \cdots \mathbb{P}\{\log_2(1 + \gamma_{N-1}) < \psi\} \mathbb{P}(\log_2(1 + \gamma_N) < \rho). \end{aligned} \quad (72)$$

By using Proposition 1 for the outage probability of each event, the result follows.

APPENDIX H

DIVERSITY OF SELECTION-BASED SCHEMES

Once again, we use the approximated expression in Theorem 2 with $T = 1$. For the TD scheme, we have

$$\Pi_{\text{TD}}(\rho) \approx (\Pi_{\text{RRC}}^{\text{CLT}}(\rho, 1))^N = \left(1 - \exp\left(-\frac{\theta\sigma^2}{MP}\right)\right)^N, \quad (73)$$

and so

$$\lim_{P \rightarrow \infty} (\Pi_{\text{RRC}}^{\text{CLT}}(\rho, 1))^N \approx \left(\frac{\theta\sigma^2}{MP}\right)^N \rightarrow O(1/P^N), \quad (74)$$

which follows from $\exp(-x) \approx 1 - x$ for $x \approx 0$. Thus, the selection-based TD scheme achieves diversity order N , with an array gain equal to (38). Next, we derive the diversity order of the coherent TD case. At the high SNR regime, $\Pi_{\text{TDCT}}(\rho)$ is dominated by the first term of the sum, that is,

$$\begin{aligned} \lim_{P \rightarrow \infty} \Pi_{\text{TDCT}}(\rho) &\approx \left(\frac{1}{\pi} \int_0^\infty \Im \left(\phi_H(t) (-1)^{2m+1} \left(j\sqrt{\frac{\theta\sigma^2}{P}} \right)^{2m} \frac{t^{2m-1}}{(2m)!} dt \right) \right)^N \\ &= \left(\frac{1}{\pi} \int_0^\infty \Im \left(\phi_H(t) (-1)^{m+1} \left(\frac{\theta\sigma^2}{P} \right)^m \frac{t^{2m-1}}{(2m)!} dt \right) \right)^N \rightarrow O(1/P^{mN}), \end{aligned} \quad (75)$$

which gives diversity of order mN , as expected. Then, after some algebraic simplifications, the array gain of this scheme is given by (39).

REFERENCES

- [1] Z. Zhang, Y. Xiao, Z. Ma, M. Xiao, Z. Ding, X. Lei, G. K. Karagiannidis, and P. Fan, "6G wireless networks: Vision, requirements, architecture, and key technologies," *IEEE Veh. Tech. Mag.*, vol. 14, no. 3, pp. 28–41, Sept. 2019.
- [2] E. Basar, M. Di Renzo, J. de Rosny, M. Debbah, M.-S. Alouini, and R. Zhang, "Wireless communications through reconfigurable intelligent surfaces," *IEEE Access*, vol. 7, pp. 116753–116773, Aug. 2019.
- [3] C. Liaskos, S. Nie, A. Tsioliaridou, A. Pitsillides, S. Ioannidis, and I. Akyildiz, "A new wireless communication paradigm through software-controlled metasurfaces," *IEEE Commun. Mag.*, vol. 56, no. 9, pp. 162–169, Sep. 2018.
- [4] M. Di Renzo et al., "Smart radio environments empowered by reconfigurable AI meta-surfaces: An idea whose time has come," *EURASIP J. Wireless Commun. Netw.*, 2019.
- [5] Q. Wu and R. Zhang, "Intelligent reflecting surface enhanced wireless network via joint active and passive beamforming," *IEEE Trans. Wireless Commun.*, vol. 18, no. 11, pp. 5394–5409, Nov. 2019.
- [6] Q. Nadeem, A. Kammoun, A. Chaaban, M. Debbah, M.-S. Alouini, "Asymptotic analysis of large intelligent surface assisted MIMO communication," [Online]. Available: <https://arxiv.org/abs/1903.08127>
- [7] E. Basar, "Reconfigurable intelligent surface-based index modulation: A new beyond MIMO paradigm for 6G," [Online]. Available: <https://arxiv.org/abs/1904.06704>
- [8] Z. Ding and H. V. Poor, "A simple design of IRS-NOMA transmission," [Online]. Available: <https://arxiv.org/abs/1907.09918>

- [9] Y. Han, W. Tang, S. Jin, C.-K. Wen, and X. Ma, "Large intelligent surface-assisted wireless communication exploiting statistical CSI," *IEEE Trans. Veh. Tech.*, vol. 68, no. 8, pp. 8238–8242, June 2019.
- [10] Z. Chu, W. Hao, P. Xiao, and J. Shi, "Intelligent reflecting surface aided multi-antenna secure transmission," *IEEE Wireless Commun. Lett.*, to be published.
- [11] M. Cui, G. Zhang, and Rui Zhang, "Secure wireless communication via intelligent reflecting surface," *IEEE Wireless Commun. Lett.*, vol. 8, no. 5, pp. 1410–1414, May 2019.
- [12] C. Huang, A. Zappone, G. C. Alexandropoulos, M. Debbah, and C. Yuen, "Reconfigurable intelligent surfaces for energy efficiency in wireless communication," *IEEE Trans. Wireless Commun.*, vol. 18, no. 8, pp. 4157–4170, Aug. 2019.
- [13] E. Bjornson, O. Ozdogan, and E. G. Larsson, "Intelligent reflecting surface vs. decode-and-forward: How large surfaces are needed to beat relaying?," *IEEE Wireless Commun. Lett.*, to be published.
- [14] T. Hou, Y. Liu, Z. Song, X. Sun, Y. Chen, and L. Hanzo, "MIMO assisted networks relying on large intelligent surfaces: A stochastic geometry model," [Online]. Available: <https://arxiv.org/abs/1910.00959>
- [15] M. Jung, W. Saad, Y. Jang, G. Kong, and S. Choi, "Performance analysis of large intelligent surfaces (LISs): Asymptotic data rate and channel hardening effects," [Online]. Available: <https://arxiv.org/abs/1810.05667>
- [16] Q. Wu and R. Zhang, "Weighted sum power maximization for intelligent reflecting surface aided SWIPT," [Online]. Available: <https://arxiv.org/abs/1907.05558>
- [17] C. Pan, H. Ren, K. Wang, M. ElKashlan, A. Nallanathan, J. Wang, and L. Hanzo, "Intelligent reflecting surface aided MIMO broadcasting for simultaneous wireless information and power transfer," [Online]. Available: <https://arxiv.org/abs/1908.04863>
- [18] R. Pedarsani, O. Leveque, and S. Yang, "On the DMT optimality of time-varying distributed rotation over slow fading relay channels," *IEEE Trans. Wireless Commun.*, vol. 14, no. 1, pp. 421–434, Jan. 2015.
- [19] R. Mudumbai, J. Hespanha, U. Madhow, and G. Barriac, "Distributed transmit beamforming using feedback control," *IEEE Trans. Inf. Theory*, vol. 56, no. 1, pp. 411–426, Jan. 2010.
- [20] C. Psomas and I. Krikidis, "Backscatter communications for wireless powered sensor networks with collision resolution," *IEEE Wireless Commun. Lett.*, vol. 6, no. 5, pp. 650–653, Oct. 2017.
- [21] I. S. Gradshteyn and I. M. Ryzhik, *Table of Integrals, Series, and Products*. Elsevier, 2007.
- [22] N. Jindal, "MIMO broadcast channels with finite-rate feedback," *IEEE Trans. Inf. Theory*, vol. 52, no. 11, pp. 5045–5060, Nov. 2016.
- [23] S. Yang and J.-C. Belfiore, "On the diversity of Rayleigh product channels," in *Proc. Int. Symp. Inf. Theory*, Nice, France, Jun. 2017.
- [24] M. Uysal, "Diversity analysis of space-time coding in cascaded Rayleigh fading channels," *IEEE Commun. Lett.*, vol. 10, no. 3, pp. 165–167, Mar. 2006.
- [25] S. Yang and J.-C. Belfiore, "Distributed rotation recovers spatial diversity," in *Proc. Int. Symp. Inf. Theory*, Austin, TX, Jun. 2010.
- [26] H. Yang and M.-S. Alouini, *Order Statistics in Wireless Communications: Diversity, Adaptation, and Scheduling in MIMO and OFDM Systems*. Cambridge University Press, 2011.
- [27] J. D. Griffin and G. D. Durgin, "Gains for RF tags using multiple antennas," *IEEE Trans. Antennas Propagat.*, vol. 56, no. 2, pp. 563–570, Feb. 2008.
- [28] J. Gil-Pelaez, "Note on the inversion theorem," *Biometrika*, vol. 38, no. 3–4, pp. 481–482, Dec. 1951.
- [29] H.-C. Yang and M.-S. Alouini, "Performance analysis of multibranch switched diversity systems," *IEEE Trans. Commun.*, vol. 51, no. 5, pp. 782–794, May 2003.